JOURNAL OF APPLIED ELECTROCHEMISTRY 11 (1981) 525–530

Postbreakdown reanodization of tantalum†

J. M. ALBELLA, I. MONTERO, M. FERNÁNDEZ, J. M. MARTÍNEZ-DUART

Departamento Fisica Aplicada and Instituto Fisica Estado Sólido, C-XII Universidad Autónoma, Cantoblanco, Madrid-34, Spain

Received 6 October 1980

The scintillation phenomenon in anodic tantalum oxide has been studied by means of the potential rise during the reoxidation of samples which had undergone previous scintillation for a specified time. The information given by these curves, together with measurements of the dielectric properties, X-ray analysis and observation under the scanning electron microscope, allow two different processes to be distinguished during scintillation. The first stage of the scintillation is mainly characterized by a process of attack and partial healing of the oxide film with the formation of pores and microfissures. The second stage of scintillation is dominated by the process of field crystallization which irreversibly degrades the oxide's dielectric properties. The influence of the anodization parameters, such as current density and nature and concentration of the electrolyte, on the above processes is also investigated.

1. Introduction

The scintillation phenomenon, i.e. dielectric breakdown during anodization of valve metals, has an important technical significance since it establishes a limit for the maximum voltage attainable in the anodic oxidation process. This voltage is strongly influenced by the anodization parameters and especially by the particular electrolyte employed, and, therefore, a significant effort has been made by the electrolytic capacitor industry to find those electrolytes which result in a high scintillation voltage [1].

There are several papers dealing with the electron injection and avalanche mechanisms which give rise to the initiation of the oxide's dielectric breakdown during anodization [2, 3]. Less attention has been directed, however, to the process of oxide recrystallization which arises as a consequence of the scintillation. The recrystallization, generally attributed to a temperature rise localized in the breakdown areas, is often described as an unwanted effect which irreversibly degrades the oxide's dielectric characteristics. Although the recrystallization has been thoroughly characterised in tantalum and aluminium oxides by optical and electron microscopy [4], there is a lack of quantitative data on the anodization parameters which control the recrystallization process. In this work we study the influence of the anodization current density and of the electrolyte's nature and concentration on the different processes which occur during scintillation of anodic tantalum oxide.

2. Experimental

Samples of tantalum foil of 99.96% purity were washed and degreased following standard procedures. Afterwards, the samples were chemically polished in a 5:2:2 mixture of H_2SO_4, HNO_3 and HF acids for 15 s. They were then treated with a solution of NH_4F in HF (300 g dm^{-3}) for 15 min. Finally the samples were thoroughly washed in deionized boiling water. These treatments leave the tantalum surface with a very low concentration of impurities, especially of fluoride ions [5, 6].

The anodization and reanodization experiments were carried out in an electrolytic cell provided with two Hewlett Packard 6209B power supplies connected in series and a stainless steel cathode. The tantalum was anodized at a constant current until the breakdown voltage was reached and the sample was left at this voltage for a specified time (scintillation time). Following this procedure, the samples were reanodized at the same current density (as programmed in the power supply). The fast increase in voltage and the initial

† Part of this work has been presented to the 8th International Vacuum Congress and the 4th International Conference on Solid Surfaces, Cannes (1980).

0021–891X/81/040525–06$02.60/0

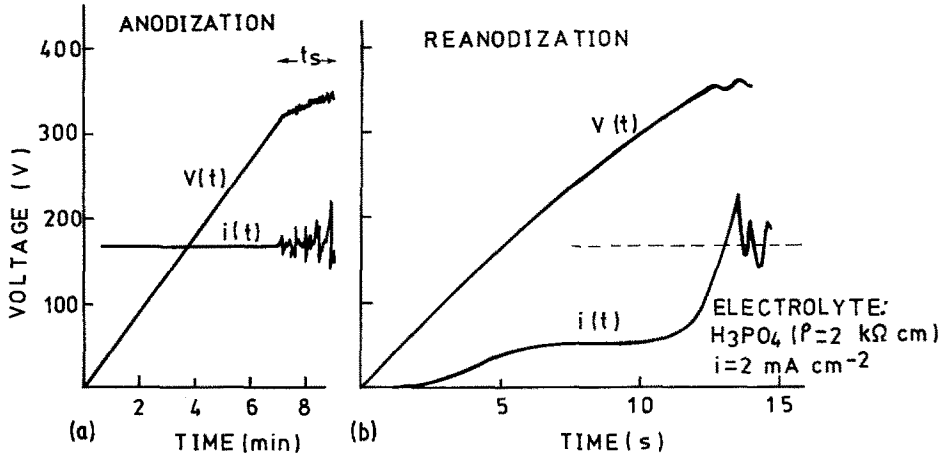

Fig. 1. Evolution of voltage and current for tantalum samples during (a) anodization followed by breakdown and (b) reanodization.

current transients were recorded in a double-channel Yew 3047 recorder. A typical plot of the variation of the voltage and current during the anodization, breakdown and reanodization processes is shown in Fig. 1. After a given scintillation time, the capacitance and associated parallel resistance of the samples were measured at 100 Hz by means of an LCR bridge, Hewlett Packard 4261A. The leakage current was also measured by polarizing the samples for 15 min at a voltage of 100 V.

By means of a protective device, only a circular section ($\sim 1\ cm^2$ in area) of the tantalum foil was in contact with the electrolyte. This avoided spurious breakdown effects at the foil's edges and at the contact between the foil and the electrolyte surface [7].

3. Results

In the reanodization experiments, after the sample had been under scintillation for a time t_s, the voltage increased with time in a nonlinear fashion. Following an initial fast increase, the rate dV/dt subsequently decreased until breakdown was reached. Parallel to this, the current across the sample was very low during the first stage; it then started to increase slowly and finally, from the time of the initiation of breakdown, acquired the value programmed by the power supply (see Fig. 1b).

A possible interpretation of the reanodization curves of Fig. 1b is that the first stage corresponds to the building of the potential difference across the equivalent resistance of the oxide layer. A number of pores, caused by the previous scintillation and whose depth is always smaller than the oxide thickness, must be repaired. However, the reanodization of the thinner oxide areas (which correspond mainly to pores and fissures) would result in a slower rate of voltage increase, which becomes essentially zero at the breakdown voltage.

In order to evaluate the rate of voltage increase after each sample has been subjected to scintillation for time t_s, the quotient $v = \Delta V/i\Delta t$ in the interval 0–250 V, where i is the current density programmed by the power supply, has been estimated. The current density has been included in the denominator for the purpose of comparing the results obtained with different current densities.

Fig. 2 represents, for different current densities, the relation v/v_0, where v_0 is the reanodization rate for $t_s = 0$, as a function of Q_s, the charge per unit area consumed during scintillation ($Q_s = it_s$). Each point of the curves of Fig. 2 corresponds to a different sample, except for the points on the 2 mA cm^{-2} curve which were obtained using the same sample subjected to alternate processes of scintillation and reanodization. The results of Fig. 2 were obtained with an electrolyte consisting of dilute aqueous H_3PO_4 (resistivity = $3.1 \times 10^3\ \Omega$ cm). The curves show an approximately

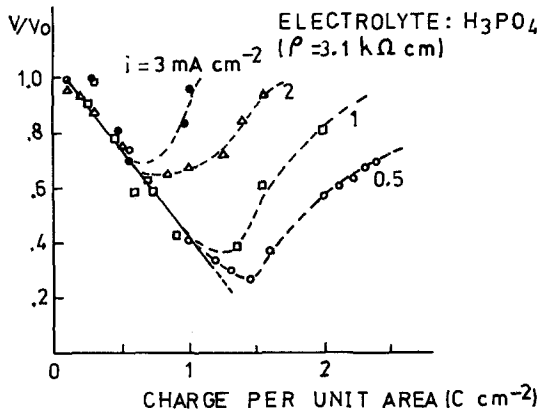

Fig. 2. Reanodization rates as a function of the charge consumed during scintillation for several anodization current densities.

linear decrease of the relative reanodization rate v/v_0 with Q_s until a minimum is reached. Its position depends strongly on the current density.

The curves of Fig. 3 show the effect of the electrolyte's resistivity (ρ) on the reanodization rate. These curves were taken at a constant current density of 2 mA cm^{-2} using aqueous H_3PO_4 electrolytes with resistivities in the range 100 to 4400 Ω cm. It can be appreciated from these curves that the minimum in the reanodization rate is markedly influenced by the electrolyte's resistivity. Other electrolytes, commonly employed in the manufacture of solid tantalum capacitors, were also investigated. These electrolytes are based on mixtures of aqueous citric and phosphoric acids in the case of low-voltage applications, and on a mixture of the same acids plus ethylene glycol for high-voltage uses [8]. The behaviour of v/v_0 versus Q_s

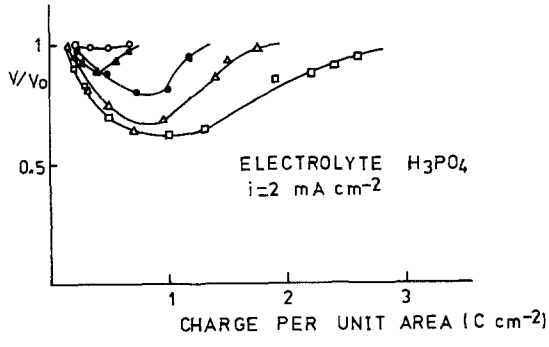

Fig. 3. Reanodization rates as a function of the charge consumed during scintillation for several electrolyte resistivities. ○, 0.1 kΩ cm; ▲, 1.0 kΩ cm, ●, 1.2 kΩ cm; △, 3.0 kΩ cm; □, 4.4 kΩ cm.

for these electrolytes, with $\rho = 100$ Ω cm, yielded similar results to those of the curve in Fig. 3 corresponding to the lowest resistivity for the phosphoric acid electrolyte.

After a given time of scintillation, the surface of the samples was examined under the scanning electron microscope and X-ray analyses were performed to determine if a possible recrystallization of the oxide had taken place. In the common descending part of the curves of Fig. 2, corresponding to the first stage of scintillation, the surface presented isolated pores and microfissures, some with ramifications, while the rest of the sample showed the normal homogeneous aspect of the amorphous oxide. By the time the minimum of the curve is reached the start of the formation of grey (recrystallized) oxide is observed, growing radially at different locations on the sample and covering wide zones of the sample after long scintillation times. Typical microphotographs of the surface are shown in Fig. 4 for each of the stages described. The X-ray diffraction analysis showed the presence of several crystalline phases of Ta_2O_5 when the samples were covered with the grey oxide, while the b.c.c. structure of the base tantalum appeared during the first stage of scintillation.

It is difficult to give an estimation of the percentage of recrystallized oxide formed during scintillation since it is very irregularly distributed. However, it is interesting to observe that the addition of ethylene glycol, in the correct amount, to the standard electrolytes based on phosphoric and citric acids strongly inhibits the grey oxide formation. The most beneficial concentration of ethylene glycol is about 25%. Higher concentrations of ethylene glycol (60% or higher) have practically no influence in avoiding the oxide's recrystallization [8].

The variation of the dielectric characteristics with scintillation time (represented by the charge Q_s) is shown in Figs. 5 and 6 for a typical case in which the electrolyte employed was a solution of H_3PO_4 ($\rho = 2200$ Ω cm) and for a current density of 2 mA cm^{-2}. The capacitance and leakage current show a minimum for a value of Q_s between 0.4 and 0.5 C cm^{-2}, whereas the associated parallel resistance shows a maximum at this value (Fig. 5). The initial decrease observed in Fig. 5 for the capacitance is probably attributed to a small oxide growth during the first stage of

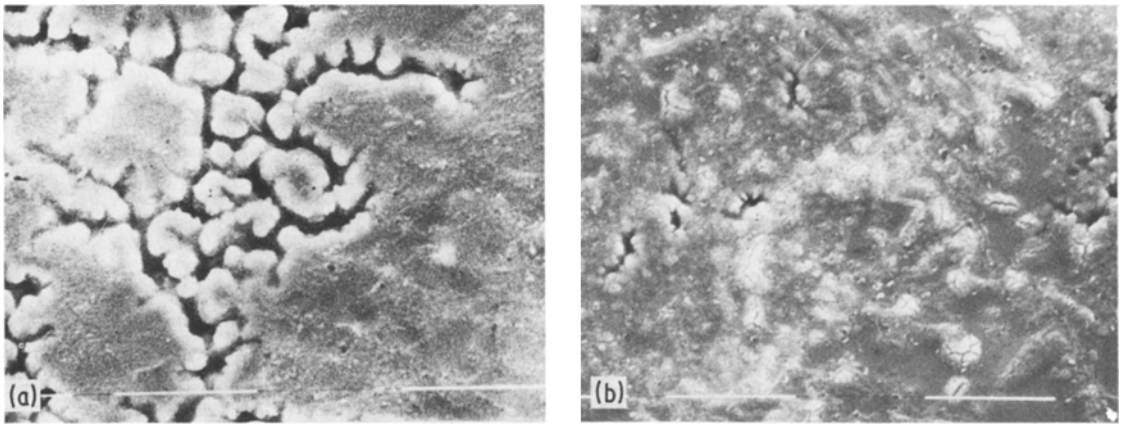

Fig. 4. Typical SEM photomicrographs of the tantalum oxide surface subjected to scintillation: (a) pores and microfissures in the oxide film; (b) recrystallized oxide (reticule 10 μm).

scintillation. This assumption is based on the changes observed in the interference colour of the oxide film as well as a small increase in the voltage from the power supply during the first part of the scintillation process. The increase in capacitance, the reduction in the associated parallel resistance and the strong enlargement of the leakage current, which occur for $Q_s > 0.5$ C cm^{-2} in the curves of Figs. 5 and 6, have necessarily to be attributed to the presence of the recrystallized oxide which was discussed earlier. In this case, the effective thickness of the blocking oxide film (amorphous oxide) diminishes and at the same time the leakage current reaches a high value as a consequence of the boundaries and fissures that develop between the polycrystalline grains and the interfaces between the crystallized and amorphous areas.

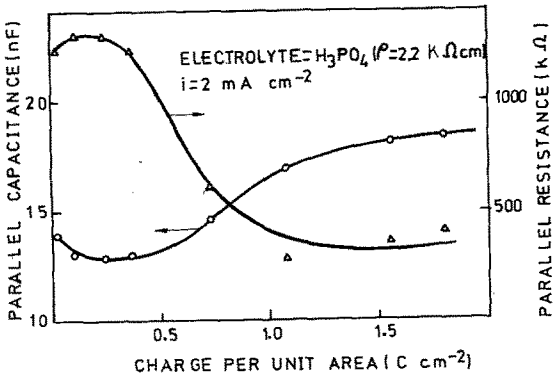

Fig. 5. Capacitance and equivalent parallel resistance as a function of the charge consumed during scintillation.

4. Discussion

The data presented for the reanodization rates, together with the observations of the oxide's structure, show that during the first stage of the scintillation phenomenon (up to the minimum in the curves of Figs. 2 and 3) an effect due to attack and partial healing of the oxide film predominates, with the formation of pores and microfissures, the number of which increases with scintillation time. The initial points of attack have sometimes been correlated with the presence of impurities at the surface as well as other kinds of defects [5].

The very nearly linear decrease of v/v_0, corresponding to the first stage of scintillation, can be explained by assuming that the number of pores produced is proportional to Q_s, which is equivalent to supposing that the production of each pore consumes the same amount of charge. When the number of pores is relatively large, the above assumption has proven to be very useful in explaining the evolution of the number of current pulses and the build up of the potential across the oxide film during scintillation [9]. Therefore, to a first approximation, it can be established that the electric potential increase during the reoxidation of the oxide layer after scintillation is given by the expression

$$\Delta V/\Delta t = k\,(i - i_{rp}) \qquad (1)$$

where k is a reanodization constant when there are no pores in the oxide and i_{rp} is the current density employed for the reoxidation of the pores. Writing

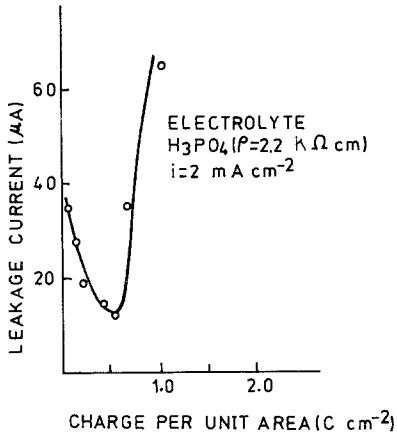

Fig. 6. Leakage current as a function of the charge consumed during scintillation.

$i_{rp} = n_p i_p$, where n_p is the concentration of pores and i_p the current density through each pore, and since, in agreement with our former assumption, $n_p = \lambda Q_s$, with λ a constant [9], Equation 1 can be expressed as

$$\Delta V/\Delta t = k(i - \lambda Q_s i_p). \quad (2)$$

Dividing both sides of Equation 2 by ki (the rate of potential growth for pore-free oxide) we have:

$$v/v_0 = 1 - \lambda (i_p/i) Q_s \quad (3)$$

which shows that the ratio v/v_0 decreases approximately linearly with Q_s during the first stage of scintillation, in agreement with the results of Fig. 2.

The occurrence of the minimum and the reversal of the slopes in the curves of Figs. 2 and 3 can be associated with the formation of crystalline oxide in a large amount. The recrystallization soon degrades the oxide's dielectric characteristics, as was observed in the discussion of the results of Figs. 5 and 6. It is also interesting to point out that the recrystallized oxide is not susceptible to being reanodized and that the crystallites mainly appear at the breakdown sites, as has been observed by Vermilyea [10] and Yahalom and Zahavi [4] using different electrolytes. In addition, as observed by Vermilyea [10], the field crystallization for voltages below breakdown requires the consumption of a certain charge, of the order of 0.4–0.5 C, the amount of which varies inversely with the electric field strength across the oxide. As a matter of fact, this result could very well explain the sequence of the curves of Fig. 2 since the electric field in the oxide increases with the anodization current density [11]. All the results just described give good evidence of the origin of the recrystallization phenomenon, which should be attributed to the electric field. Other explanations about the origin of the crystallization of the amorphous oxide, such as being solely due to Joule heating during anodization, should be disregarded [4], although obviously a temperature rise during anodization would accelerate the field crystallization effect.

The effect of the electrolyte concentration on the scintillation is also very significant. In effect, as can be appreciated from the curves of Fig. 3, the initial decrease of v/v_0 versus Q_s is somewhat similar for all the electrolytes, but the upturn branches appear at lower values of Q_s as the resistivity of the electrolyte gets smaller. In this respect it should be mentioned that although Jackson [12] has found that the field crystallization effect strongly increases with pH, there is a lack of studies dealing with the influence of the resistivity of the electrolyte on the recrystallization phenomenon. Recently Ikonopisov and Elenkov [13] have shown that the electrolyte concentration plays an important role in the electronic current injection across the oxide. In fact they have found an expression of the type $j_e = a\sigma^b$ for the dependence of the electronic current density j_e on the conductivity σ of the electrolyte (a and b are constants). Although more experimentation will be necessary to elucidate the effect of the electrolyte on scintillation, it can in principle be assumed that the rate of field crystallization would be controlled by the electronic current injected into the oxide and therefore it could be expected that the rate of crystallization would increase with j_e.

References

[1] F. J. Burger and L. Young, in 'Progress in Dielectrics' Vol. 5 (edited by J. Birks and J. Hart) Academic Press, New York (1962).
[2] S. Ikonopisov, *Electrochim. Acta* **22** (1977) 1077.
[3] V. Kadary and N. Klein, *J. Electrochem. Soc.* **127** (1980) 139.
[4] J. Yahalom and J. Zahavi, *Electrochim. Acta* **16** (1971) 603.
[5] J. M. Albella, M. J. Puente, J. Baonza, M. T. Martin-Patino and J. M. Martinez-Duart, *Proc. 7th Int. Vacuum Congress and 3rd Int. Conf. on Solid Surfaces, Vienna* (1977) p. 2055.
[6] B. Maurel, D. Dieumegard and G. Amsel, *J. Elec-*

Electrochem. Soc. **119** (1972) 1715.
[7] J. M. Albella, I. Montero, J. Baonza and J. M. Martinez-Duart, *Electrocomp. Sci. Technol.* (in press).
[8] M. Fernández, J. Baonza, J. M. Albella and J. M. Martinez-Duart, *ibid* in press.
[9] J. M. Albella, I. Montero and J. M. Martinez-Duart, *Thin Solid Films* **58** (1979) 307.
[10] D. A. Vermilyea, *J. Electrochem. Soc.* **102** (1955) 207.
[11] L. Young, 'Anodic Oxide Films', Academic Press, New York (1961).
[12] N. F. Jackson, *J. Appl. Electrochem.* **3** (1973) 91.
[13] S. Ikonopisov and N. Elenkov, *J. Electroanal. Chem.* **86** (1978) 105.